European Radiology (2021) 31:7696–7704
https://doi.org/10.1007/s00330-021-07898-7

GASTROINTESTINAL

Macrotrabecular-massive hepatocellular carcinoma: imaging identification and prediction based on gadoxetic acid–enhanced magnetic resonance imaging

Jie Chen[1] · Chunchao Xia[1] · Ting Duan[1] · Likun Cao[2] · Hanyu Jiang[1] · Xijiao Liu[1] · Zhen Zhang[1] · Zheng Ye[1] · Zhenru Wu[3] · Ronghui Gao[1] · Yujun Shi[3] · Bin Song[1]

Received: 7 February 2021 / Revised: 6 March 2021 / Accepted: 16 March 2021 / Published online: 15 April 2021

Abstract

Objectives To identify image features of macrotrabecular-massive (MTM) hepatocellular carcinoma (HCC) and to determine its role in predicting MTM-HCC.

Methods Patients who underwent preoperative gadoxetic acid-enhanced MRI and with surgery proven HCC were retrospectively included. Imaging features were assessed according to Liver Imaging Reporting and Data System. Quantitative measurements were recorded. Clinical characteristics and imaging findings were compared between MTM-HCCs and non-MTM-HCCs. Predictive factors of MTM-HCC were screened with univariate analyses and then identified with multivariate logistic regression. A regression-based diagnostic model was constructed. ROC analyses were used to determine cutoff values, AUC, and corresponding 95% confidence interval (CI) of findings. The diagnostic performance was validated by 10-fold cross-validation.

Results One hundred and forty-one patients with 37 MTM-HCCs were included. Multivariate analyses identified high platelet count ($\geq 163.5 \times 10^3$/ul, odds ratio = 3.20; 95% CI: 1.29, 7.96; $p = 0.012$), low tumor-to-liver ADC ratio (≤ 1.05, odds ratio = 3.05; 95% CI, 1.23 - 7.55; $p = 0.016$), and necrosis or severe ischemia (odds ratio = 11.61; 95% CI, 3.99 - 33.76, $p < 0.001$) as independent predictors of MTM-HCC. Necrosis or severe ischemia alone helped identify 86% MTM-HCCs with a specificity of 66%. The average AUCs were 0.81 (95% CI: 0.71, 0.90) for the regression-based diagnostic model, with a sensitivity of 57% and specificity of 92%.

Conclusions Necrosis or severe ischemia was a sensitive imaging feature of MTM-HCC. Noninvasive prediction of this subtype can be achieved with good accuracy and excellent specificity when findings were combined.

Key Points

- *The macrotrabecular-massive (MTM) hepatocellular carcinoma (HCC) represents an aggressive subtype of HCC and is associated with poor prognosis.*
- *Imaging features of necrosis or severe ischemia alone helped identify 86% MTM-HCCs with a specificity of 66%.*
- *A regression-based diagnostic model including high platelet count ($\geq 163.5 \times 10^3$/ul), low tumor-to-liver ADC ratio (≤ 1.05), and necrosis or severe ischemia can provide noninvasive assessment of MTM-HCC with good accuracy and high specificity.*

Keywords Carcinoma, hepatocellular · Magnetic resonance imaging · Nomogram

Jie Chen and Chunchao Xia contributed equally to this work.

✉ Yujun Shi
shiyujun@scu.edu.cn

✉ Bin Song
songlab_radiology@163.com

[1] Department of Radiology, West China Hospital, Sichuan University, No.37 Guoxue Alley, Chengdu 610041, China

[2] Department of Radiology, Peking Union Medical College Hospital (Dongdan campus), No.1 Shuaifuyuan Wangfujing Dongcheng District, Beijing 100730, China

[3] Laboratory of Pathology, West China Hospital, Sichuan University, No.88 South Keyuan Road, Chengdu 610041, China

Abbreviations

ADC	Apparent diffusion coefficient
APF	Alpha-fetoprotein
AUC	Area under the ROC curve
CI	Confidence interval
cv.AUC	Cross-validated AUC
HBP	Hepatobiliary phase
HBV	Hepatitis B virus
HCC	Hepatocellular carcinoma
LI-RADS	Liver Imaging Reporting and Data System
MTM	Macrotrabecular-massive
ROC	Receiver operating characteristic
SI	Signal intensity

Introduction

Hepatocellular carcinoma (HCC) remains one of the major causes of cancer-related death [1]. Despite improved patient management over the last decade, clinical outcomes of HCC patients are poor and vary a lot, with a large proportion of patients diagnosed at advanced stages, and patients eligible for curative therapies suffer from high rates of tumor recurrence [2]. The reported recurrence rate varies between 40% and 80% within 5 years of surgical resection [3].

Patient stratification according to different molecular or pathological characteristics might be beneficial [4, 5]. Several major HCC subtypes have been proposed, such as steatohepatic subtype, scirrhous subtype, and fibrolamellar subtype. However, the clinical application of those tumor classifications is limited either due to their low expression rates or vague prognosis value [6]. Recently, a newly identified histological subtype, designated as "macrotrabecular-massive hepatocellular carcinoma" (MTM-HCC), has been catching attention. It has been shown tightly associated with more aggressive biological and molecular features, such as high alpha-fetoprotein (AFP) levels, TP53 mutations, larger tumor size, satellite nodules, and vascular invasion. Prior studies also suggested that MTM-HCC was a strong independent prognostic predictor of early and overall recurrence [7, 8]. Its prognostic value was retained even after patient stratification according to tumor size, Barcelona Clinic Liver Cancer stage, satellite nodules, and vascular invasion [8]. The identification of this aggressive HCC subtype is therefore expected to hold promise for personalized treatment and prognosis prediction.

Since biopsy is not required for the diagnosis of HCC, imaging has turned out to be an especially useful method for noninvasive diagnosis and characterization of HCC. Tumors with different histopathological features might have different pathways of carcinogenesis and subsequently show different imaging features [9]. For example, imaging features defined by the Liver Imaging Reporting and Data System (LI-RADS), which provides standardized terminology for liver imaging evaluation, have shown excellent performance in identifying HCC with progenitor phenotype [10]. The significant angiogenesis activation in MTM-HCC may also result in specific imaging features [11, 12].

In east countries, chronic hepatitis B virus (HBV) infection is the main risk factor of HCC, and it accounts for at least 50% of cases of HCC worldwide [13]. For improved sensitivity of HCC detection, the acquisition of hepatobiliary phase (HBP) image using hepatocyte-specific contrast agent, such as gadoxetic acid, has been recommended by multiple Asian guidelines [14–16]. However, imaging features of MTM-HCC in the east population, especially with the extra acquisition of HBP images, have not been fully investigated. Prior studies indicated that imaging features of necrosis and arterial phase hypovascular component can help identifying MTM-HCC, both with high sensitivity but low specificity [17, 18].

Therefore, the purpose of this study is to identify imaging features that can help differentiate MTM-HCC from non-MTM-HCCs based on gadoxetic acid-enhanced MRI and to determine its diagnostic performance in predicting MTM-HCC.

Materials and methods

Study participants

This retrospective study was approved by the Institutional Review Board and written informed consent was waived. The study protocol conforms to the ethical guidelines of the 1975 Declaration of Helsinki as reflected in a priori approval by the institution's human research committee. From August 2015 to December 2018, 307 consecutive patients with preoperative gadoxetic acid-enhanced MRI and subsequent tumor resection were originally retrieved. Exclusion criteria were non-HCC lesions, prior anti-tumoral treatment, recurrent tumor, unavailable tumor specimens for pathological analyses, small lesions (≤ 1 cm), and poor imaging quality. Flowchart of retrospective patient selection is displayed in Fig. 1. Other clinical and biological information include gender, age, background liver diseases, serum tumor biomarkers, and liver function test.

Pathological analysis

One pathologist (Y.S.) with 20 years of experience in liver pathology reviewed all histological slides without the awareness of other clinical and imaging results. According to previous criteria, tumors with a predominant (> 50%) macrotrabecular (trabecular of more than six cells thick) architecture pattern were classified as MTM-HCC [8]. Tumor differentiation according to the Edmondson-Steiner criteria and liver cirrhosis were also evaluated.

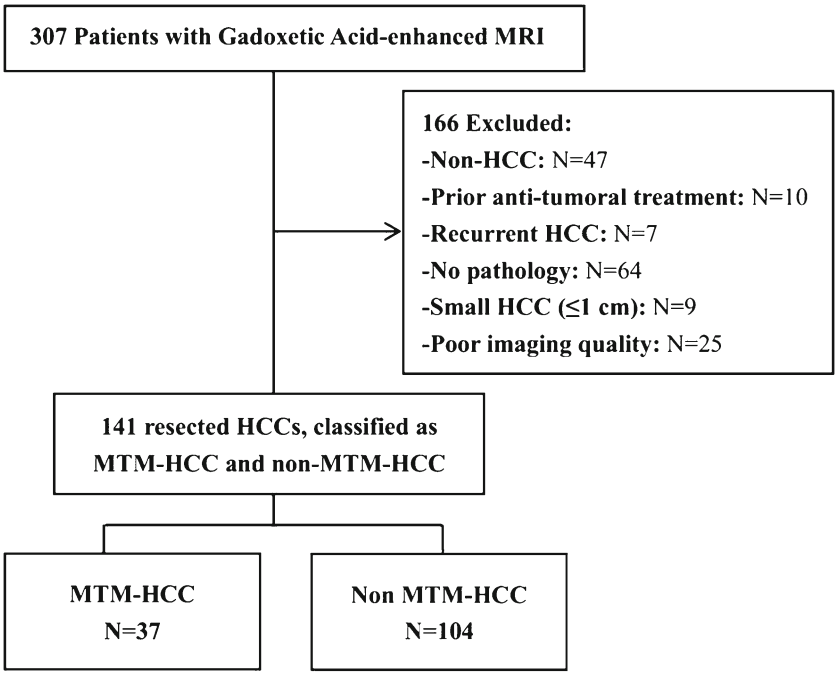

Fig. 1 Chart flow of retrospective patient selection for the evaluation of macrotrabecular-massive hepatocellular carcinoma (MTM-HCC)

Image acquisition

All gadoxetic acid-enhanced MRIs were performed prospectively at a 3-T scanner (Magnetom Skyra, Siemens Healthineers) with an 18-channel phase-array body coil and spine coil. The MRI protocol included axial and coronal T2-weighted imaging, in-phase and opposed-phase T1-weighted imaging, diffusion-weighted imaging, and magnetic resonance cholangiopancreatography. Gadoxetic acid was applied at a dose of 0.025 mmol/kg. Dynamic phases were acquired before and after contrast injection using voxel interpolate breath-hold fat-suppressed T1-weighted imaging. Hepatobiliary phase (HBP) was acquired 20 min after contrast injection. Apparent diffusion coefficient (ADC) map was reconstructed after data acquisition using *b* value of 0 and 800 s/mm^2. Detailed description for MRI protocol is provided in supplementary Table 1.

Image analysis

Two independent radiologists (X.L. and H.J., with 11 and 5 years of experience in liver imaging, respectively) reviewed all imaging features defined by the LI-RADS version 2018, without the awareness of other clinical and pathological results. In case of multiple liver lesions, the largest one was selected as the target lesion for both imaging and pathology analyses. Necrosis or severe ischemia was defined as areas within a solid mass which either does not enhance at all or enhances very mildly at arterial phase and portal venous phase and affecting at least 20% of the tumor at the level of the largest cross-sectional diameter. The presence of internal arteries, irregular tumor margin, and peritumoral hypointense at HBP were additionally evaluated. Discrepancies were solved with consulting a third radiologist (B.S.) for consensus. Imaging features were first screened according to prevalence. Only imaging features with prevalence between 10% and 90% were included in further analyses.

Quantitative analyses were performed by another research (J.C., with 5 years of experience in liver imaging). Briefly, a free-hand region of interest was placed on each of three successive transverse slices at the maximal transverse dimension of the tumor, avoiding intratumoral hemorrhage, and necrosis. The background liver was also evaluated with three circular regions of interest measuring 200-300 mm^2 without the inclusion of any major vasculature and artifact. Signal intensity (SI) of tumor and liver from three slices were averaged and used to calculate following variables: tumor relative enhancement at arterial phase = $[(SI_{AP} - SI_{Pre})/SI_{Pre}]$, relative enhancement at portal venous phase = $[(SI_{PVP} - SI_{Pre})/SI_{Pre}]$, tumor-to-liver SI ratio at HBP = $[SI_{HBP-HCC}/SI_{HBP-Liver}]$, and tumor-to-liver ADC ratio = $[ADC_{HCC}/ADC_{Liver}]$, where SI_{Pre}, SI_{AP}, and SI_{PVP} were the SI of HCC at pre-contrast, arterial phase, and portal venous phase, respectively; $SI_{HBP\text{-}HCC}$ and $SI_{HBP\text{-}Live}$ were SI of HCC and the background liver at HBP phase; and ADC_{HCC} and ADC_{Liver} were the ADC value of HCC and the background liver, respectively.

Statistical analysis

Continuous variables were summarized as median and interquartile and were compared between MTM-HCCs and non-MTM-HCCs using the Many-Whiney *U* test.

Table 1 Clinical and pathological characteristics of MTM-HCCs and non-MTM-HCCs

Variables	Non-MTM-HCC ($N = 104$)	MTM-HCC ($N = 37$)	p value
Age	54 (45.25 – 62.75)	47 (38.50 – 55.50)	0.005
Alpha-fetoprotein (ng/ml)	49.88 (4.73 – 741.78)	599.90 (8.60 – 1210.0)	0.009
Carcinoembryonic antigen (ng/ml)	2.26 (1.40 – 3.09)	2.09 (1.32 – 2.80)	0.534
Carbohydrate antigens 19-9 (U/ml)	18.53 (11.20 – 30.36)	18.55 (11.01 – 31.39)	0.821
Total bilirubin (umol/l)	14.05 (10.90 – 18.40)	14.00 (10.85 – 17.85)	0.840
Direct bilirubin (umol/l)	5.10 (4.03 – 6.58)	4.60 (4.05 – 7.20)	0.833
Indirect bilirubin (umol/l)	8.65 (6.53 – 12.23)	8.80 (6.75 – 12.65)	0.718
Albumin (g/l)	42.85 (40.58 – 45.20)	42.80 (40.90 – 45.10)	0.771
Prothrombin time (second)	12.20 (11.60 – 12.90)	12.00 (11.50 – 12.90)	0.762
Aspartate transaminase (IU/l)	37.00 (28.00 – 50.25)	43.00 (30.50 – 71.00)	0.064
Alanine aminotransferase (IU/l)	36.0 (22.25 – 54.0)	35.00 (24.50 – 51.50)	0.753
Platelet count ($\times 10^3$/ul)	137.00 (104.75 – 169.75)	174.0 (134.0 – 213.5)	0.003
Gender (male) [a]	83 (79.8%)	27 (73.0%)	0.389
Hepatitis B virus infection [a]	100 (95.2%)	37 (100.0%)	0.326
Cirrhosis (stage 4 fibrosis) [a]	45 (43.3%)	14 (37.8%)	0.565
Edmondson-Steiner grade [a]			0.001
I	11 (10.6%)	1 (2.7%)	
II	47 (45.2%)	7 (18.9%)	
III	37 (35.6%)	23 (62.2%)	
IV	9 (8.7%)	6 (16.2%)	

Note: Unless indicated otherwise, data are median value and data in parentheses are interquartile range. *MTM*, macrotrabecular-massive; *HCC*, hepatocellular carcinoma. [a] Data are numbers of patients, with percentages in parentheses

Binary variables were compared using the chi-square test or Fisher's exact test. Receiver operating characteristic (ROC) curves were used to determine the threshold of continuous variables in predicting MTM-HCC. A diagnostic model was constructed by including significant findings at univariate analyses into multivariate logistic regression. A nomogram was built for the model. The diagnostic performances and corresponding 95% confidence intervals (CI) of significant findings, combinations of findings, and the regression-based model were evaluated by the area under the ROC curve (AUC) and validated by 10-fold cross-validation on the same dataset. Statistical analyses were carried out by SPSS (version 22.0) and R software (version 3.5.3), and a significant level of $p < 0.05$ was used.

Results

Demographic and pathological characteristics

The final study group consists of 141 patients (110 males, 31 females), including 37 MTM-HCCs and 104 non-MTM-HCCs. The time interval between MRI scan and tumor resection ranged from 1 to 35 days (mean: 3 days). The main risk factors of liver disease were HBV infection in 136 patients

Table 2 Quantitative imaging parameters between MTM-HCCs and non-MTM-HCCs

Imaging parameters	Non-MTM-HCC ($N = 104$)	MTM-HCC ($N = 37$)	p value
Tumor size	5.25 (3.29 – 7.00)	7.43 (4.55 – 10.02)	< 0.001
Relative enhancement at arterial phase	0.57 (0.30 – 0.81)	0.33 (0.15 – 0.56)	0.002
Relative enhancement at portal venous phase	0.61 (0.51 – 0.76)	0.53 (0.42 – 0.79)	0.230
Tumor-to-liver SI ratio at HBP	0.56 (0.50 – 0.65)	0.52 (0.48 – 0.59)	0.036
Tumor-to-liver ADC ratio	1.11 (1.02 – 1.25)	1.02 (0.94 – 1.18)	0.006

Note: Data are median value and data in parentheses are interquartile range. *MTM*, macrotrabecular-massive; *HCC*, hepatocellular carcinoma; *SI*, signal intensity; *HBP*, hepatobiliary phase; *ADC*, apparent diffusion coefficient

Table 3 Comparison of qualitative imaging features between MTM-HCCs and non-MTM-HCCs

Imaging features	Non-MTM-HCC (N = 104)	MTM-HCC (N = 37)	p value
Marked T2 hyperintensity	61 (58.7%)	32 (86.5%)	0.002
Non-rim APHE	88 (84.6%)	31 (83.8%)	0.905
Multifocality	27 (26.0%)	8 (21.6%)	0.600
Necrosis or severe ischemia	35 (33.7%)	32 (86.5%)	< 0.001
Internal arteries	26 (25.0%)	21 (56.8%)	< 0.001
Blood product in mass	45 (43.3%)	25 (67.6%)	0.011
Targetoid appearance	17 (16.3%)	13 (35.1%)	0.016
Infiltrative appearance	12 (11.5%)	8 (21.6%)	0.131
Absent or incomplete capsule	74 (71.2%)	37 (100.0%)	< 0.001
Enhancing capsule	65 (62.5%)	25 (67.6%)	0.582
Tumor in vein	18 (17.3%)	10 (27.0%)	0.203
Corona enhancement	34 (32.7%)	22 (59.5%)	0.004
Nodule in nodule	66 (63.5%)	20 (54.1%)	0.314
Mosaic architecture	67 (64.4%)	32 (86.5%)	0.012
Fat in mass, more than adjacent liver	40 (38.5%)	17 (45.9%)	0.426
Irregular tumor margin	44 (42.3%)	17 (45.9%)	0.701
Peritumoral hypointense at HBP	42 (40.4%)	21 (56.8%)	0.085
Image cirrhosis	47 (45.2%)	13 (35.1%)	0.288

Note: Data are number of patients, with percentages in parentheses. *MTM*, macrotrabecular-massive; *HCC*, hepatocellular carcinoma; *APHE*, arterial phase hyperenhancement; *HBP*, hepatobiliary phase

(96.5%), coinfection of hepatitis B and hepatitis C virus in 2 patients, autoimmune hepatitis in 1 patient, nonalcoholic fatty liver disease in 1 patient, and undetermined in other 3 patients. Baseline clinical and histopathological characteristics of patients and tumors were summarized in Table 1. Generally, patients with MTM-HCCs were younger, with higher AFP levels, higher platelet count, and higher tumor histological grades. Other information did not show significant differences between MTM-HCCs and non-MTM-HCCs.

Imaging findings

Quantitative analyses (Table 2) revealed significantly larger tumor size, lower relative enhancement at arterial phase, lower tumor-to-liver SI ratio at HBP, and lower tumor-to-liver ADC ratio, in MTM-HCCs. At qualitative analysis (Table 3), MTM-HCCs more frequently showed marked T2 hyperintensity, necrosis or severe ischemia, internal arteries, blood product in mass, targetoid appearance, absent or incomplete tumor capsule, corona enhancement, and mosaic architecture. Representative images of MTM-HCCs are demonstrated in Figs. 2 and 3.

The best cutoff value to predict MTM-HCC was estimated to be ≤ 50 years old in age, ≥ 110 ng/ml for AFP level, ≥ 40 U/L for aspartate transaminase, ≥ 163.5 × 10^3/ul for platelet count, ≥ 7.4 cm for tumor size, ≤ 0.64 for relative enhancement at arterial phase, and ≤ 1.05 for tumor-to-liver ADC ratio, respectively, according to corresponding ROC analyses. Multivariable analyses identified platelet count ≥ 163.5 × 10^3/

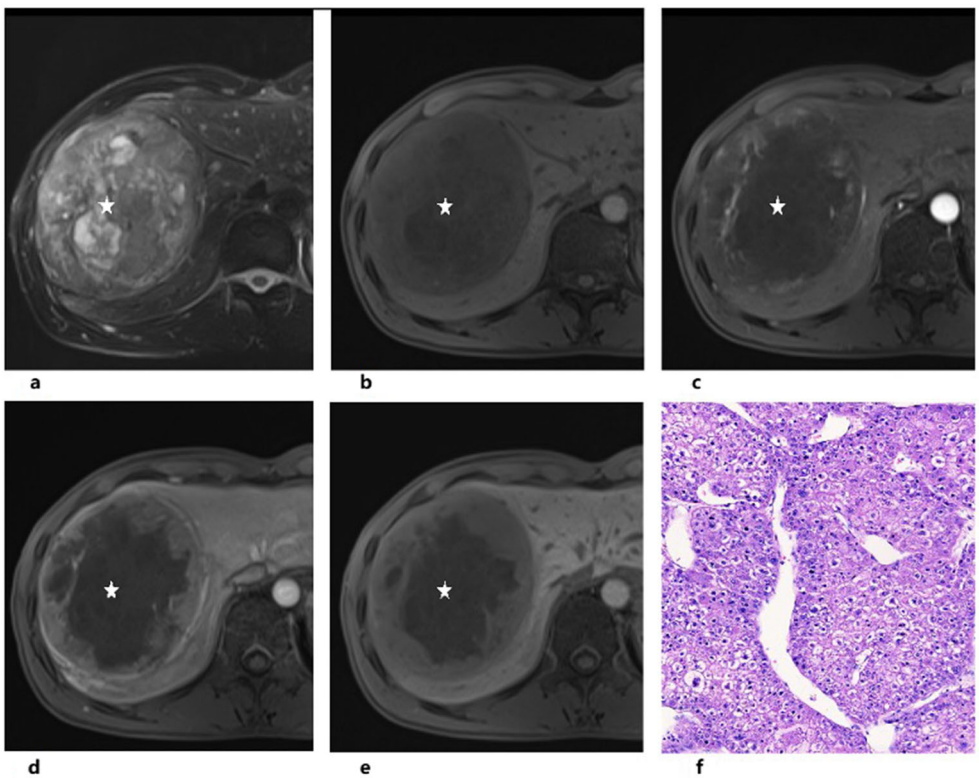

Fig. 2 Imaging features of macrotrabecular-massive hepatocellular carcinoma (MTM-HCC) in a 32-year-old man with hepatitis B virus infection. Necrosis (star) appears as mixed T2 hyperintensity (**a**) and T1 hypointensity (**b**), and does not enhance at all at arterial (**c**), portal venous (**d**), and hepatobiliary phase (**e**). Traveling arteries were evident at peripheral tumor at arterial phase (**c**). Incomplete capsule was observed at portal venous phase (**d**). Tumor showed predominant thick trabecular architecture at pathological evaluation (**f**, hematoxylin-eosin stain, original magnification, ×100)

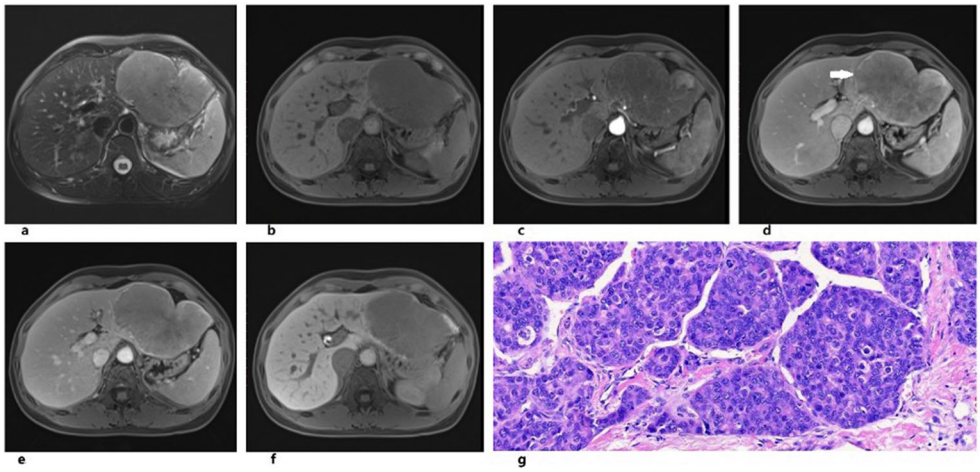

Fig. 3 Imaging features of macrotrabecular-massive hepatocellular carcinoma (MTM-HCC) in a 32-year-old woman with hepatitis B virus infection. No substantial necrosis was observed at T2-weighted imaging (**a**) and pre-contrast T1-weighted imaging (**b**), however, tumor showed only mild enhancement at arterial (**c**) and portal venous (**d**) phases, consistent with severe ischemia. Incomplete enhancing capsule (white arrow) was also observed at portal venous phase (**d**). Delayed central enhancement was observed at delayed phase (**e**). No significant finding was found at the hepatobiliary phase (**f**). Tumor was classified as MTM-HCC at hematoxylin-eosin stain (**g**, original magnification, ×100)

ul (odds ratio = 3.20; 95% CI, 1.29-7.96; $p = 0.012$), tumor-to-liver ADC ratio ≤ 1.05 (odds ratio = 3.05; 95% CI, 1.23 - 7.55; $p = 0.016$), and necrosis or severe ischemia (odds ratio = 11.61; 95% CI, 3.99 - 33.76, $p < 0.001$) as independent predictor of MTM-HCCs.

Diagnostic performance

Diagnostic performances of each significant finding at multivariable analysis, combinations of findings, and the constructed regression model in predicting MTM-HCCs are summarized in Table 4. Necrosis or severe ischemia alone identified 86% (32/37) of MTM-HCCs with a specificity of 66% and a cross-validated AUC (cv.AUC) of 0.76. When any two criteria were satisfied, the sensitivity, specificity, and cv.AUC were 0.78, 0.77, and 0.77, respectively. When all three criteria were satisfied, the sensitivity, specificity, and cv.AUC were 0.30, 0.97, and 0.63, respectively. The sensitivity, specificity, and cv.AUC of the regression-based model were 0.57, 0.92, and 0.81, respectively. Compared with single finding and straightforward combinations of findings, the regression-based model demonstrated higher AUCs. Nomogram of the regression-based model is shown in Fig. 4.

Discussion

The newly defined morphological subtype of macrotrabecular-massive hepatocellular carcinoma (MTM-HCC) represents an aggressive form of HCC and exhibited strong prognostic significance [8]. Recent studies showed that MTM-HCCs were strongly associated with frequent early recurrence and poor disease-specific survival in both resected and radiofrequency ablation-treated HCCs [7, 8]. Therefore, the identification of MTM-HCC before treatment, especially local regional treatment, may provide useful prognostic information. It might also prompt more intensive follow-up strategy. As biopsy is not required for diagnosing HCC, noninvasive imaging identification of this subtype is therefore of paramount importance for both therapeutic and prognostic purpose.

Table 4 Diagnostic performances of each finding, combination of findings, and the regression-based model in predicting MTM-HCCs

Criteria/models	Sensitivity	Specificity	PPV	NPV	Accuracy	AUC	cv.AUC
Platelet count ≥ 163.5 × 10^3/ul	0.57	0.72	0.42	0.82	0.68 (0.60 – 0.76)	0.64 (0.55 – 0.74)	0.65 (0.50 – 0.79)
Tumor-to-liver ADC ratio ≤ 1.05	0.59	0.68	0.40	0.83	0.66 (0.58 – 0.73)	0.64 (0.55 – 0.73)	0.63 (0.49 – 0.77)
Necrosis or severe ischemia	0.86	0.66	0.48	0.93	0.72 (0.63 – 0.79)	0.76 (0.69 – 0.84)	0.76 (0.63 – 0.89)
Any two criteria	0.78	0.77	0.55	0.91	0.77 (0.70 – 0.84)	0.78 (0.70 – 0.86)	0.77 (0.64 – 0.91)
All three criteria	0.30	0.97	0.79	0.80	0.79 (0.72 – 0.86)	0.63 (0.56 – 0.71)	0.63 (0.44 – 0.82)
Regression-based model	0.57	0.92	0.72	0.86	0.83 (0.76 – 0.89)	0.84 (0.76 – 0.92)	0.81 (0.71 – 0.90)

Note: Numbers in parentheses are 95% confidence intervals. *MTM*, macrotrabecular-massive; *HCC*, hepatocellular carcinoma; *ADC*, apparent diffusion coefficient, *AUC*, area under the receiver operating characteristic curve; *cv.AUC*, average AUC at 10-fold cross-validation

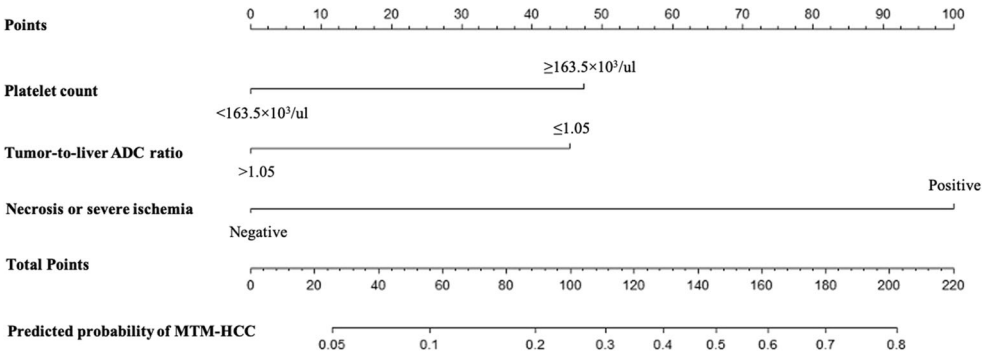

Fig. 4 Nomograms of the regression-based model. Predictor points are found on an uppermost point scale that corresponds to each variable. On the bottom scale, points for all variables are added and translated into the provability of hepatocellular carcinoma with macrotrabecular-massive subtype

Our study identified high platelet count, low tumor-to-liver ADC ratio, and necrosis or severe ischemia as independent predictors of MTM-HCCs. Necrosis or severe ischemia sensitively identified 86% of MTM-HCCs with a specificity of 66%. When findings were combined, MTM-HCC can be identified with high specificity. Moreover, our study also indicated a limited role of the hepatobiliary phase for the prediction of MTM-HCC.

The expression rate of MTM-HCCs among all HCCs in this study (26.2%, 37/141) is higher than previous studies (16%-17%) [8, 17], with also predominantly higher rate of HBV infection (96.5% vs. 22.4%). According to a recent study, MTM-HCC was more frequent in patients with HBV infection [19]. Despite huge difference in the background liver diseases, the result of our study was consistent with the recently reported substantial necrosis in MTM-HCC, which was thought to be related to the angiogenesis activation in peripheral tumor [7, 8, 11, 12], favoring central necrosis due to rapidly reduced central perfusion [17]. In this study, the image feature of necrosis or severe ischemia was more sensitive than specific to MTM-HCC. This can be explained by the trade-off between sensitivity and specificity when extra consideration was given to severe ischemia, which will eventually result in tumor necrosis.

From a clinical perspective, a suspicion based on imaging markers would need to be confirmed by biopsy if the diagnosis might eventually interfere with treatment decisions. In this setting, the high sensitivity of necrosis or ischemia might be preferred over the previously reported high specificity of substantial necrosis [17] in clinical practice. As a result of ischemia in fast-growing tumor, necrosis is commonly seen in advanced HCC. Accordingly, tumor size was higher in MTM-HCC in this study.

Our study also found more frequent internal arteries and blood product in mass in MTM-HCC, which we speculate, might be features in response to vascular sprouting and subsequent intratumoral hemorrhage caused by blood vessel destabilization [20, 21]. We ended up with few references on this topic. Rhee et al recently also reported intratumoral artery as ancillary findings indicative of MTM-HCC [18]. Tumor growth pattern could be another explanation. According to previous studies, blood vessels tend to be retained with the infiltrating replacement growth pattern in intrahepatic cholangiocarcinoma [22, 23]. Likewise, this also applies to HCC with infiltrating growth. In this study, infiltrating appearance was more frequent in MTM-HCC, though the difference was not significant. We should also mention that despite angiogenesis activation, relative tumor enhancement at arterial phase is lower in MTM-HCC. The tumor-to-liver ADC ratio was also lower in MTM-HCC. This is in keeping with previous conclusion about decreased arterial supply and more restricted diffusion in more aggressive HCCs [9]. In this study, high-grade (Edmondson-Steiner grades III and IV) tumor was significantly more frequent in MTM-HCC (78.4% vs. 44.3%).

Other imaging findings in MTM-HCC included absent or incomplete capsule, corona enhancement, and mosaic architecture. Those imaging findings are all indicative of aggressive tumor biological behaviors, such as poor differentiation, stemness, vascular invasion, and tumor recurrence [9, 10, 24]. The more frequent mosaic architecture feature is in agreement with previously reported more tumor heterogeneity in MTM-HCC [17]. Moreover, although peritumoral hypointense at HBP was more frequent in MTM-HCC, no HBP-related finding was retained after multivariate analyses, indicating that for the prediction of MTM-HCC, the supplementary value of extra HBP image was limited.

High platelet count ($\geq 163.5 \times 10^3$/ul) was identified as predictive factors of MTM-HCC in this study. To the best of our interpretation, the higher level of platelet count in MTM-HCC might also be related to its distinctively activated angiogenesis [11]. As a key driving force for angiogenesis, vascular endothelial growth factor is largely sequestered and mainly transported by the blood platelet in the circulation [25]. Various studies have explored the relation between platelet count and HCC, with no consensus reached yet [26].

Certain limitations in this study should be acknowledged. First, selection bias might exist in this retrospective study, with the inclusion of only surgery resected liver lesions. Therefore, results from this study might not be able to represent the whole clinical spectrum. Second, a substantial number of cases (n = 25) were excluded due to poor image quality (mostly due to severe motion-related artifacts in the arterial phase). By

including only good quality images, the diagnostic accuracy could be overestimated. Second, the sample size is relatively small in this study, and we were unable to perform an external validation due to the single-center design. Alternatively, an internal 10-fold cross-validation was performed. Therefore, the conclusion of this study needs to be verified by larger multicentric studies.

In conclusion, this study revealed necrosis or severe ischemia as a sensitive imaging feature of macrotrabecular-massive hepatocellular carcinoma. Noninvasive prediction of this subtype can be achieved with good accuracy and excellent specificity when findings were combined.

Supplementary Information The online version contains supplementary material available at https://doi.org/10.1007/s00330-021-07898-7.

Funding This study has received funding from the National Nature Science Foundation of China (Grant Number 81771797) and Science and Technology Support Program of Sichuan Province (Grant Number 2017SZ0003).

Declarations

Guarantor The scientific guarantor of this publication is Bin Song (songlab_radiology@163.com, Tel: +86 189-8060-1592, No.37 Guoxue Alley, Chengdu, 610041, China).

Conflict of interest The authors of this manuscript declare no relationships with any companies whose products or services may be related to the subject matter of the article.

Statistics and biometry No complex statistical methods were necessary for this paper.

Informed consent Written informed consent was waived by the Institutional Review Board.

Ethical approval Institutional Review Board approval was obtained.

Methodology
- Retrospective
- Diagnostic or prognostic study
- Performed at one institution

References

1. Siegel RL, Miller KD (2020) Cancer statistics, 2020. CA Cancer J Clin 70:7–30
2. Kumari R, Sahu MK, Tripathy A, Uthansingh K, Behera M (2018) Hepatocellular carcinoma treatment: hurdles, advances and prospects. Hepat Oncol 5:Hep08
3. Portolani N, Coniglio A, Ghidoni S et al (2006) Early and late recurrence after liver resection for hepatocellular carcinoma: prognostic and therapeutic implications. Ann Surg 243:229–235
4. Uenishi T, Kubo S, Yamamoto T et al (2003) Cytokeratin 19 expression in hepatocellular carcinoma predicts early postoperative recurrence. Cancer Sci 94:851–857
5. Guan DX, Shi J, Zhang Y et al (2015) Sorafenib enriches epithelial cell adhesion molecule-positive tumor initiating cells and exacerbates a subtype of hepatocellular carcinoma through TSC2-AKT cascade. Hepatology 62:1791–1803
6. Torbenson MS (2017) Morphologic subtypes of hepatocellular carcinoma. Gastroenterol Clin North Am 46:365–391
7. Calderaro J, Couchy G, Imbeaud S et al (2017) Histological subtypes of hepatocellular carcinoma are related to gene mutations and molecular tumour classification. J Hepatol 67:727–738
8. Ziol M, Poté N, Amaddeo G et al (2018) Macrotrabecular-massive hepatocellular carcinoma: a distinctive histological subtype with clinical relevance. Hepatology 68:103–112
9. Yoneda N, Matsui O, Kobayashi S et al (2019) Current status of imaging biomarkers predicting the biological nature of hepatocellular carcinoma. Jpn J Radiol 37:191–208
10. Chen J, Wu Z, Xia C et al (2020) Noninvasive prediction of HCC with progenitor phenotype based on gadoxetic acid-enhanced MRI. Eur Radiol 30:1232–1242
11. Calderaro J, Meunier L, Nguyen CT et al (2019) ESM1 as a marker of macrotrabecular-massive hepatocellular carcinoma. Clin Cancer Res 25:5859–5865
12. Renne SL, Woo HY, Allegra S et al (2020) Vessels encapsulating tumor clusters (VETC) is a powerful predictor of aggressive hepatocellular carcinoma. Hepatology 71:183–195
13. Xie Y (2017) Hepatitis B virus-associated hepatocellular carcinoma. Adv Exp Med Biol 1018:11–21
14. Kumar A, Acharya SK, Singh SP et al (2020) 2019 Update of Indian National Association for study of the liver consensus on prevention, diagnosis, and management of hepatocellular carcinoma in India: the Puri II Recommendations. J Clin Exp Hepatol 10:43–80
15. Kudo M, Matsui O, Izumi N et al (2014) JSH consensus-based clinical practice guidelines for the management of hepatocellular carcinoma: 2014 update by the Liver Cancer Study Group of Japan. Liver Cancer 3:458–468
16. Omata M, Cheng AL, Kokudo N et al (2017) Asia-Pacific clinical practice guidelines on the management of hepatocellular carcinoma: a 2017 update. Hepatol Int 11:317–370
17. Mulé S, Galletto Pregliasco A, Tenenhaus A et al (2020) Multiphase liver MRI for identifying the macrotrabecular-massive subtype of hepatocellular carcinoma. Radiology 295:562–571
18. Rhee H, Cho ES, Nahm JH et al (2021) Gadoxetic acid-enhanced MRI of macrotrabecular-massive hepatocellular carcinoma and its prognostic implications. J Hepatol 74:109–121
19. Jeon Y, Benedict M, Taddei T, Jain D, Zhang X (2019) Macrotrabecular hepatocellular carcinoma: an aggressive subtype of hepatocellular carcinoma. Am J Surg Pathol 43:943–948
20. Zhang L, Yang N, Park JW et al (2003) Tumor-derived vascular endothelial growth factor up-regulates angiopoietin-2 in host endothelium and destabilizes host vasculature, supporting angiogenesis in ovarian cancer. Cancer Res 63:3403–3412
21. Gerald D, Chintharlapalli S, Augustin HG, Benjamin LE (2013) Angiopoietin-2: an attractive target for improved antiangiogenic tumor therapy. Cancer Res 73:1649–1657
22. Tsunematsu S, Chuma M, Kamiyama T et al (2015) Intratumoral

artery on contrast-enhanced computed tomography imaging: differentiating intrahepatic cholangiocarcinoma from poorly differentiated hepatocellular carcinoma. Abdom Imaging 40:1492–1499
23. Miura F, Okazumi S, Takayama W et al (2004) Hemodynamics of intrahepatic cholangiocarcinoma: evaluation with single-level dynamic CT during hepatic arteriography. Abdom Imaging 29:467–471
24. Nishie A, Asayama Y, Ishigami K et al (2014) Clinicopathological significance of the peritumoral decreased uptake area of gadolinium ethoxybenzyl diethylenetriamine pentaacetic acid in hepatocellular carcinoma. J Gastroenterol Hepatol 29:561–567
25. Hashiguchi T, Arimura K, Matsumuro K et al (2000) Highly concentrated vascular endothelial growth factor in platelets in Crow-Fukase syndrome. Muscle Nerve 23:1051–1056
26. Aryal B, Yamakuchi M, Shimizu T et al (2018) Deciphering platelet kinetics in diagnostic and prognostic evaluation of hepatocellular carcinoma. Can J Gastroenterol Hepatol 2018:9142672